The Journal of Immunology

RESEARCH ARTICLE | SEPTEMBER 15 2017

Macrophages Induce Long-Term Trapping of γδ T Cells with Innate-like Properties within Secondary Lymphoid Organs in the Steady State

Alexandra Audemard-Verger; ... et. al

J Immunol (2017) 199 (6): 1998–2007.
https://doi.org/10.4049/jimmunol.1700430

Macrophages Induce Long-Term Trapping of γδ T Cells with Innate-like Properties within Secondary Lymphoid Organs in the Steady State

Alexandra Audemard-Verger,*,[1] Matthieu Rivière,*,[1] Aurélie Durand,*,[1] Elisa Peranzoni,* Vincent Guichard,*,† Pauline Hamon,‡ Nelly Bonilla,* Thomas Guilbert,* Alexandre Boissonnas,‡ Cédric Auffray,* Gérard Eberl,§,¶ Bruno Lucas,*,[2] and Bruno Martin*,[2]

So far, peripheral T cells have mostly been described to circulate between blood, secondary lymphoid organs (SLOs), and lymph in the steady state. This nomadic existence would allow them to accomplish their surveying task for both foreign Ags and survival signals. Although it is now well established that γδ T cells can be rapidly recruited to inflammatory sites or in certain tumor microenvironments, the trafficking properties of peripheral γδ T cells have been poorly studied in the steady state. In the present study, we highlight the existence of resident γδ T cells in the SLOs of specific pathogen-free mice. Indeed, using several experimental approaches such as the injection of integrin-neutralizing Abs that inhibit the entry of circulating lymphocytes into lymph nodes and long-term parabiosis experiments, we have found that, contrary to Ly-6C$^{-/+}$CD44^{lo} and Ly-6C^{+}CD44^{hi} γδ T cells, a significant proportion of Ly-6C^{-}CD44^{hi} γδ T cells are trapped for long periods of time within lymph nodes and the spleen in the steady state. Specific in vivo cell depletion strategies have allowed us to demonstrate that macrophages are the main actors involved in this long-term retention of Ly-6C^{-}CD44^{hi} γδ T cells in SLOs. ***The Journal of Immunology*****, 2017, 199: 1998–2007.**

The γδ T cells are unique and distinct from other lymphocyte subsets, such as NK cells, B cells, and αβ T cells, in that they combine adaptive features with rapid, innate-like responses that allow them to play an important role in all phases of an immune response. γδ T cells are crucially involved in host immune defense against infections (1) but are also known to have a strong clinical association with various autoimmune diseases such as inflammatory bowel disease (2, 3), rheumatoid arthritis (or collagen-induced arthritis, the murine model of rheumatoid arthritis) (4, 5), and multiple sclerosis (or experimental autoimmune encephalomyelitis, the murine model of multiple sclerosis) (6, 7).

Additionally, there is compelling evidence to indicate that γδ T cells play an important role in immunity to cancer by sensing and reacting to cellular stress. This has been clearly demonstrated in murine models of spontaneous (8), chemically induced (9), transgenic (10), and transplantable tumors (11, 12). However, it seems that the activity of γδ T cells in response to tumors can differ radically according to the tumor type or environment (13, 14). These data may actually reflect the high diversity of the γδ T cell compartment.

In this regard, we have recently shown that within murine secondary lymphoid organs (SLOs), γδ T cells can be subdivided into four subsets according to CD44 and Ly-6C expression. More precisely, we have characterized the functional heterogeneity of the peripheral γδ T cell compartment that comprises Ly-6C^{-}CD44^{hi} γδ T cells exhibiting innate-like features and naive and memory adaptive-like γδ T cells (Ly-6C$^{-/+}$CD44^{lo} γδ T cells and Ly-6C^{+}CD44^{hi} γδ T cells, respectively) (15).

This phenotypic and functional heterogeneity of the peripheral γδ T cell compartment may be also associated with differential T cell trafficking dynamic properties. So far, peripheral T cells are mostly described to circulate between blood, SLOs, and lymph in the steady state. This nomadic existence would allow them to accomplish their surveying task for both foreign Ags and survival signals (16, 17). In line with this concept, Mandl et al. (18) have shown in a recent study that the mean transit time for CD4^{+} and CD8^{+} αβ T cells in peripheral lymph nodes (pLNs) were 12 and 18 h, respectively. Concerning γδ T cells, it is now well established that γδ T cells can be rapidly recruited to inflammatory sites or to certain tumor microenvironments (19, 20). These γδ T cell infiltrations are notably orchestrated by inflammatory cytokines such as IL-1β or IL-23 or chemokine axes such as CCL2/CCR2 (12, 21–23). However, the T cell trafficking dynamics of peripheral γδ T cell subsets in the steady state have still been poorly studied.

In this study, using several experimental approaches such as the injection of integrin-neutralizing Abs that inhibit the entry of

*Institut Cochin, CNRS UMR8104, INSERM U1016, Paris Descartes Université, 75014 Paris, France; †Paris Diderot Université, 75013 Paris, France; ‡Université Paris 6, INSERM U1135, CNRS ERL8255, Centre d'Immunologie et des Maladies Infectieuses, Sorbonne Universités, Université Pierre et Marie Curie, 75013 Paris, France; §Unité Microenvironment and Immunity, Institut Pasteur, 75724 Paris, France; and ¶INSERM U1224, 75724 Paris, France

[1]A.A.-V., M.R., and A.D. contributed equally to this work.

[2]B.L. and B.M. contributed equally to this work.

ORCIDs: 0000-0002-7770-7210 (A.B.); 0000-0002-0322-3977 (B.L.).

Received for publication March 24, 2017. Accepted for publication July 10, 2017.

This work was supported by grants from the Ligue contre le Cancer, the Association pour la Recherche contre le Cancer, and the Fondation pour la Recherche Médicale. M.R. was supported by a fellowship from the Fondation pour la Recherche Médical. A.A.-V. and P.H. were supported by a Ph.D. fellowship from the Ligue contre le Cancer and from INSERM. V.G. was supported by a Ph.D. fellowship from the French Ministry of National Education, Research, and Technology. E.P. was supported by a fellowship from the Fondation de France.

Address correspondence and reprint requests to Dr. Bruno Martin, Cochin Institute, 27 rue du Faubourg Saint Jacques, 75014 Paris, France. E-mail address: bruno.martin@inserm.fr

The online version of this article contains supplemental material.

Abbreviations used in this article: DC, dendritic cell; DT, diphtheria toxin; LN, lymph node; mLN, mesenteric LN; pLN, peripheral LN; ROR, retinoic acid–related orphan receptor; SLO, secondary lymphoid organ.

circulating lymphocytes into LNs and long-term parabiosis experiments, we have found that contrary to Ly-6C$^+$ CD44^{hi} and CD44^{lo} γδ T cell subsets, which are circulating cells, an important proportion of Ly-6C$^-$CD44^{hi} γδ T cells is residing within SLOs in the steady state. Moreover, specific in vivo cell depletion strategies have allowed us to demonstrate that macrophages are the main actors involved in this long-term trapping of Ly-6C$^-$CD44^{hi} γδ T cells in SLOs in the steady state.

Materials and Methods

Mice

C57BL/6 CD45.1 mice, C57BL/6 CD45.2 mice, C57BL/6 μMT mice, and C57BL/6 CD11c.DTR mice (24) were maintained in our own animal facilities, under specific pathogen-free conditions. C57BL/6 retinoic acid–related orphan receptor (ROR)γt-GFP mice were initially obtained from Dr. G. Eberl (Institut Pasteur, Paris, France) (25). Six- to 12-wk-old mice were used for experiments. Animal housing, care, and research were carried out in accordance with the guidelines of the French Veterinary Department. All procedures were approved by the French Animal Experimentation and Ethics Committee and validated by the Service Protection et Santé Animales, Environnement (numbers C-75-562 and A-75-1315). Sample sizes were chosen to assure reproducibility of the experiments and in accordance with the 3Rs of animal ethics regulation (i.e., replacement, reduction, and refinement).

Cell suspensions

pLNs (pooled cervical, axillary, brachial, and inguinal LNs), mesenteric LNs (mLNs), cervical LNs, and spleen were homogenized and passed through a nylon cell strainer (BD Falcon) in RPMI 1640 GlutaMAX (Life Technologies) supplemented with 10% FCS (Biochrom) for adoptive transfer and cell culture (LNs only), or in 5% FCS, 0.1% NaN_3 (Sigma-Aldrich) in PBS for flow cytometry.

To verify the efficiency of dendritic cell (DC) or macrophage in vivo depletion, LNs and spleens were disrupted in RPMI 1640 medium containing 5% FCS, 1 mg of collagenase from *Clostridium histolyticum* type II and type IV (Sigma-Aldrich), and 0.5 mg of DNase I (Sigma-Aldrich) and incubated for 20 min at 37°C.

Fluorescence staining and flow cytometry

Cell suspensions were collected and dispensed into 96-well round-bottom microtiter plates (6×10^6 cells per well; Greiner Bioscience). Surface staining was performed as previously described (26, 27). Briefly, cells were incubated on ice, for 15 min per step, with Abs in 5% FCS (Biochrom), 0.1% NaN_3 (Sigma-Aldrich) in PBS. Each cell-staining reaction was preceded by a 15-min incubation with a purified anti-mouse CD16/32 Ab (FcγRII/III block; 2.4G2) obtained from hybridoma supernatants. For determination of intracellular cytokine production, cells were stimulated with 0.5 μg/ml PMA (Sigma-Aldrich), 0.5 μg/ml ionomycin (Sigma-Aldrich), and 10 μg/ml brefeldin A (Sigma-Aldrich) for 2 h at 37°C. Cells were then stained for surface markers, fixed in 2% paraformaldehyde in PBS, and permeabilized with 0.5% saponin, followed by labeling with specific cytokine Abs.

S1PR1 was detected with a rat mAb (R&D Systems). Briefly, cells were first incubated for 90 min with the anti-S1PR1 rat mAb (50 μg/ml) in PBS containing 0.5% FCS, 1 mM EDTA, 0.05% azide, and 2% normal mouse serum. After washing, cells were then incubated with donkey biotinylated anti-rat IgG polyclonal Abs (Jackson ImmunoReaserch Laboratories) for 30 min in the above medium followed by streptavidin-allophycocyanin (BioLegend).

Multicolor immunofluorescence was analyzed using BD LSR II and BD LSRFortessa cytometers (BD Biosciences). List mode data files were analyzed using FACSDiva software (BD Biosciences). Data acquisition was performed in the Cochin Cytometry and Immunobiology facility.

Parabiosis

Female host parabionts were generated with 8- to 12-wk-old C57BL/6 CD45.1 mice and C57BL/6 CD45.2 mice. The percentage of host cells in a given T cell subset corresponds to the percentage of CD45.1$^+$ cells for the CD45.1 parabiont and the percentage of CD45.2$^+$ cells for the CD45.2 parabiont.

Blocking T cell entry into LNs

Purified anti–VLA-4 (clone PS/2) and anti–LFA-1 (clone M17/4) Abs were obtained from Bio X Cell. For short-term treatment, mice were injected i.p. one time with 200 μg of both Abs and then analyzed 48 h later. For long-term treatment, mice were injected i.p. every 2 d during 6 d (four injections) with 200 μg of both Abs and analyzed 24 h later.

In vivo cell depletions

For DC depletion, C57BL/6 CD11c.DTR mice (referred to as CD11c DOG mice) were injected i.p. every 2 d during 6 d (four injections) with 250 ng of diphtheria toxin (DT).

The CSF1R inhibitor PLX3397 incorporated into rodent chow at 290 ppm (delivering daily doses of ~45 mg/kg) was provided along with control chow from Plexxikon (Berkeley, CA). For macrophage in vivo depletion, C57BL/6 mice were fed with PLX3397 or control chow during 7 d.

FTY720 treatment

Mice were injected i.p. daily with FTY720 (Cayman Chemical) in saline at a dose of ~1 μg/g during 7 d.

Immunofluorescence microscopy

Inguinal, axillary, brachial, and maxillary mouse LNs were initially fixed overnight in 0.1 M phosphate buffer containing 75 mM L-lysine, 10 mM $NaIO_4$, and 1% paraformaldehyde (PLP fixative buffer). These organs were then embedded in 5% low-gelling-temperature agarose (type VII-A; Sigma-Aldrich) prepared in PBS. LN slices (230 μm) were cut with a vibratome (VT 1000S; Leica) in a bath of ice-cold PBS. Slices were then incubated at 37°C, for 20 min per step, with Abs in PBS. Stained slices were photographed on an upright Leica stand with a confocal spinning disk Yokogawa head with a ×25/0.95 Leica objective. Acquisitions were made with a Flash 4 LT Hamamatsu camera. Analysis was performed using ImageJ software. Data acquisition was performed on the Cochin imaging photonic (IMAG'IC) facility.

In vivo LPS challenge

C57BL/6 RORγt-GFP mice were injected i.v. with 100 μg of LPS (from *Escherichia coli* 0111:B4; Sigma-Aldrich). Three hours after LPS challenge, cells recovered from pLNs, mLNs, and the spleen were incubated with 10 μg/ml brefeldin A (Sigma-Aldrich) for 2 h at 37°C for determination of intracellular cytokine production.

Statistical analysis

Data are expressed as mean ± SEM, and the significance of differences between two series of results was assessed using the Student paired or unpaired *t* test. A p value <0.05 was considered significant ($*p < 0.05$, $**p < 0.01$, $***p < 0.001$, $****p < 0.0001$).

Results

An important proportion of Ly-6C$^-$CD44^{hi} γδ T lymphocytes are trapped in LNs in the steady state

According to Ly-6C and CD44 expression, we have recently characterized the heterogeneity of the peripheral γδ T cell compartment by showing that it comprises Ly-6C$^-$CD44^{hi} γδ T cells exhibiting innate-like features and naive and memory adaptive-like γδ T cells (Ly-6C$^{-/+}$CD44^{lo} γδ T cells and Ly-6C$^+$CD44^{hi} γδ T cells, respectively) (15). To go further, we decided to study the T cell trafficking dynamics of these subsets. We first inhibited the entry of circulating lymphocytes into LNs through the injection of integrin-neutralizing Abs (18, 28, 29). More precisely, C57BL/6 mice were injected i.p. with anti–LFA-1 and anti–VLA-4 Abs (Fig. 1A). We first verified that all γδ T cells from pLNs, mLNs, and the spleen were expressing both LFA-1 and VLA-4 integrins (Supplemental Fig. 1). The phenotype of γδ T cells remaining within LNs was analyzed 48 h after initiating the treatment (Fig. 1A). Interestingly, at that time point, Ly-6C$^-$CD44^{hi} γδ T cells were greatly enriched within the γδ T cells remaining within pLNs (Fig. 1B, 1C). This resulted from the fact that the great majority of Ly-6C$^-$CD44^{hi} γδ T cells (~75%) remained trapped within pLNs whereas almost all of the other γδ T cells had egressed from them (Fig. 1D). Such a phenomenon could also be observed, to a lower extent, in mLNs, as ~15% of the Ly-6C$^-$CD44^{hi} γδ T cells were still present within this SLO 48 h after the injection of

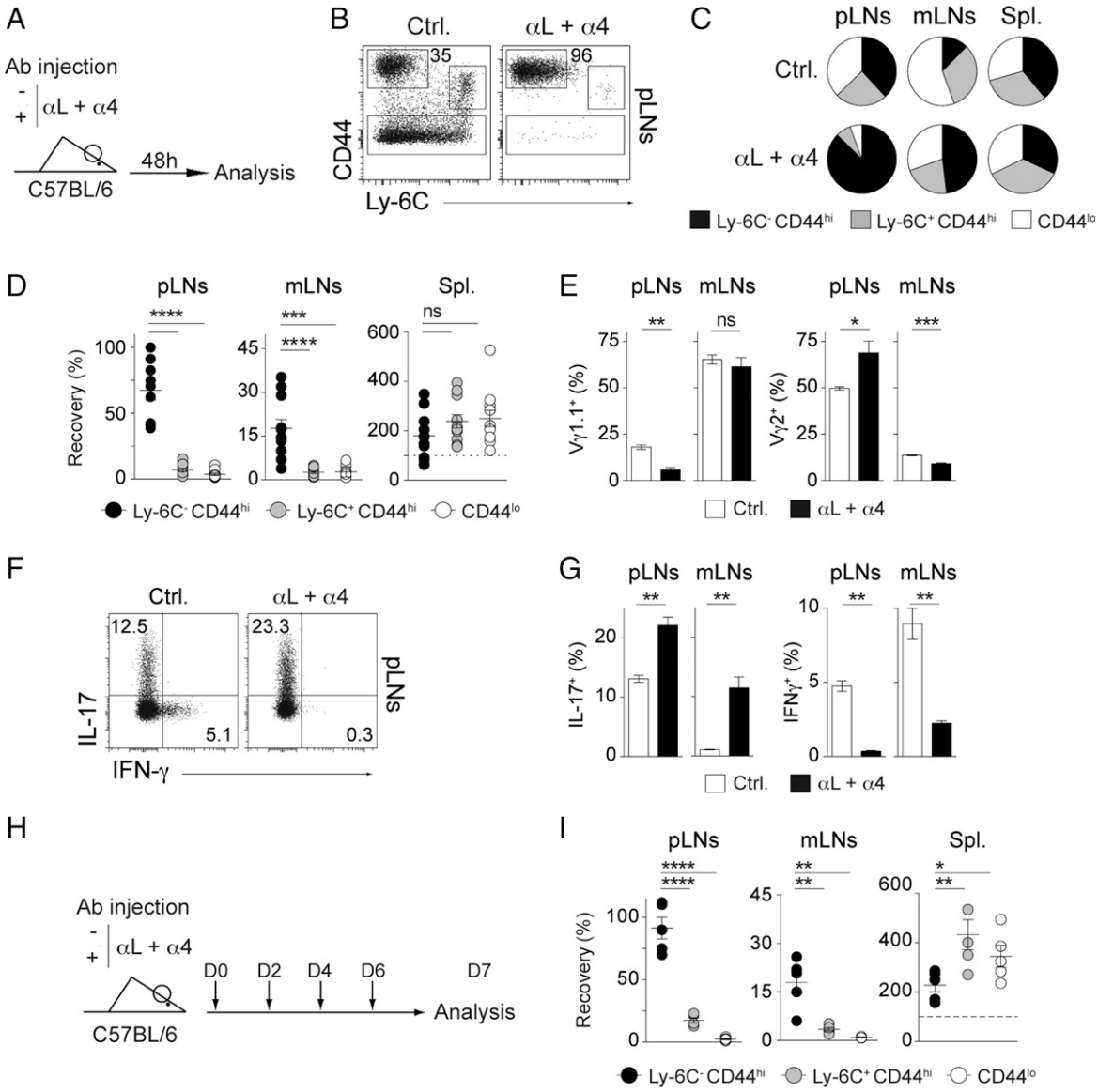

FIGURE 1. An important proportion of Ly-6C$^-$CD44^{hi} γδ T lymphocytes is trapped in LNs in the steady state. C57BL/6 mice have been injected i.p. with integrin-neutralizing anti–LFA-1 and anti–VLA-4 Abs. Two days after treatment, pLNs, mLNs, and spleen were recovered separately. (**A**) Diagram illustrating the experimental model. (**B**) CD44/Ly-6C dot plots for gated TCRγδ$^+$ cells recovered from pLNs of representative control and treated mice. Numbers on FACS dot plots indicate the percentage of Ly-6C$^-$CD44^{hi} γδ T cells among the γδ T lymphocyte compartment. (**C**) Pie charts illustrating the proportions of γδ T cell subsets recovered from pLNs, mLNs, and spleen of control and treated mice. (**D**) Percentage of γδ T cell subset recovery within pLNs, mLNs, and spleen of anti–LFA-1– and anti-VLA-4–treated mice. The percentage of recovery was calculated by dividing the absolute numbers in treated mice by the mean absolute number obtained in untreated animals. (**E**) Percentage of Vγ1.1$^+$ and Vγ2$^+$ cells among Ly-6C$^-$CD44^{hi} γδ T cells recovered from pLNs and mLNs of control and anti–LFA-1– and anti-VLA-4–treated mice. (**F**) IL-17/IFN-γ dot plots for gated TCRγδ$^+$ cells recovered from pLNs of representative control and treated mice. (**G**) Proportion of IL-17– and IFN-γ–producing TCRγδ$^+$ cells recovered from pLNs and mLNs of control and treated mice. (**H** and **I**) C57BL/6 mice have been injected i.p. every 2 d during 6 d with 200 μg of both integrin-neutralizing Abs and analyzed 24 h later. (H) Diagram illustrating the experimental model. (I) Percentage of γδ T cell subset recovery within pLNs, mLNs, and spleen of 6 d treated mice. For (C)–(E), (G), and (I), results are shown as mean ± SEM for at least two mice per group per experiment, from at least three independent experiments, and each point indicates an individual mouse. Significance of differences between two series of results was assessed using a two-tailed paired (D and H) or unpaired (C and F) Student *t* test. $*p < 0.05$, $**p < 0.01$, $***p < 0.001$, $****p < 0.0001$. α4, anti–VLA-4; Ctrl., control; αL, anti–LFA-1; Spl., spleen.

integrin-neutralizing Abs (Fig. 1C, 1D). Of note, in this model, we observed a strong increase in the absolute numbers of all the different γδ T cell subsets in the spleen (Fig. 1D). This phenomenon could result from the accumulation in the spleen of T lymphocytes egressing from LNs.

Narayan et al. (30) have previously shown that distinct cell types in the γδ T cell lineage could be identified on the basis of their TCR repertoire usage. Therefore, we then analyzed the Vγ-chain repertoire of Ly-6C$^-$CD44^{hi} γδ T cells remaining within pLNs and mLNs after the injection of integrin-neutralizing Abs (Fig. 1E). Although we noticed a decreased proportion of Vγ1.1-expressing cells associated with an enrichment of Vγ2-expressing cells within pLNs following treatment, such a discrepancy was not observed within mLNs, indicating that Vγ-chain usage does not allow precise identification of LN-trapped γδ T lymphocytes.

Consistent with the fact that Ly-6C$^-$CD44^{hi} γδ T lymphocytes are the only γδ T cells able to produce IL-17 in response to stimulation (15), we observed that, after treatment, within both

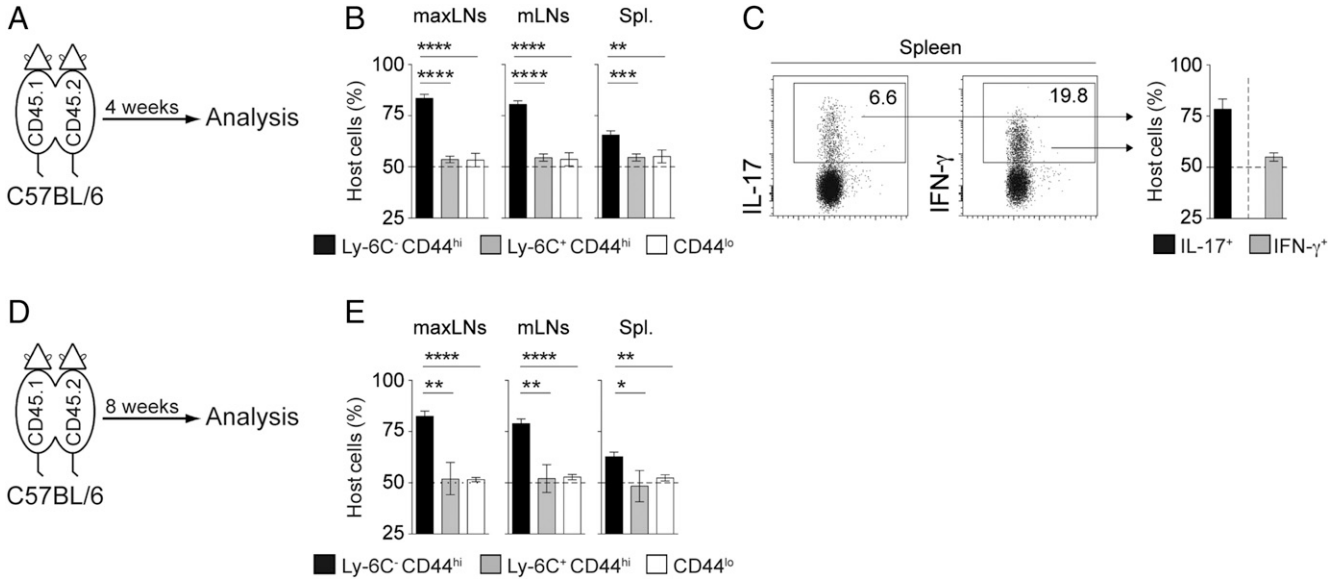

FIGURE 2. Ly-6C$^-$CD44^{hi} γδ T lymphocytes are largely long-term SLO-resident cells in the steady state. Parabiotic mice were established between CD45.1 and CD45.2 C57BL/6 mice. Four weeks after surgery, parabiotic pairs were analyzed. (**A**) Diagram illustrating the experimental model. (**B**) Proportions of host cells, CD45.1$^+$ for the CD45.1 parabiont and CD45.2$^+$ for the CD45.2 parabiont, among the indicated γδ T cell subsets recovered from pLNs, mLNs, and spleen from parabiotic pairs. (**C**) IL-17 and IFN-γ dot plots for gated TCRγδ$^+$ cells recovered from spleen of representative parabiotic mice and percentage of host cells among these IL-17– and IFN-γ–producing γδ T cells. (**D** and **E**) Parabiotic mice were established between CD45.1 and CD45.2 C57BL/6 mice and analyzed 8 wk after surgery. (D) Diagram illustrating the experimental model. (E) Proportions of host cells among the indicated γδ T cell subsets recovered from pLNs, mLNs, and spleen from parabiotic pairs. Results are shown as mean ± SEM for at least three mice per group per experiment, from at least three independent experiments. *$p < 0.05$, **$p < 0.01$, ***$p < 0.001$, ****$p < 0.0001$. Spl., spleen.

pLNs and mLNs, a clear and significant increase in the proportion of IL-17–producing γδ T cells correlated with a diminished ability of the remaining γδ T cells to produce IFN-γ (Fig. 1F, G).

Because circulatory dynamics could differ between γδ T cell subsets (i.e., Ly-6C$^-$CD44^{hi} γδ T cells could need more time to exit LNs than Ly-6C$^+$ CD44^{hi} and CD44^{lo} γδ T cells), we then decided to extend to 7 d the duration of the treatment blocking T cell entry into LNs from the blood (Fig. 1H). In this setting, we still observed that whereas almost all Ly-6C$^+$ CD44^{hi} and CD44^{lo} γδ T cells have left LNs, the great majority of Ly-6C$^-$CD44^{hi} γδ T cells were still trapped in pLNs and to a lesser extent in mLNs (Fig. 1I). Taken together, our data suggest that contrary to the other γδ T cell subsets, Ly-6C$^-$CD44^{hi} γδ T lymphocytes from LNs are in part noncirculating cells.

A significant proportion of Ly-6C$^-$CD44^{hi} γδ T lymphocytes is long-term SLO-resident cells in the steady state

To explain the results presented above, one may argue that Ly-6C$^-$CD44^{hi} γδ T cells could enter into LNs in an LFA-1– and VLA-4–independent manner. To address this issue, we then examined the cell exchange rate of the various γδ T cell subsets from SLOs (using CD45.1 and CD45.2 congenic markers) that occurred between parabiotic pairs (Fig. 2A). Four weeks following surgery, although both Ly-6C$^+$ CD44^{hi} and CD44^{lo} γδ T cells have achieved full chimerism in all studied SLOs, Ly-6C$^-$CD44^{hi} lymphocytes showed only limited exchange between the parabionts (Fig. 2B). In line with a weak circulatory dynamic of Ly-6C$^-$CD44^{hi} γδ T cells, we also observed a limited exchange of splenic IL-17–producing γδ T cells between parabiotic mice (Fig. 2C). To examine whether these results were stable over time, we performed longer term parabiosis experiments (Fig. 2D). Eight weeks after surgery, in all studied SLOs, Ly-6C$^-$CD44^{hi} γδ T lymphocytes still showed limited exchange between the paired mice (Fig. 2E). Collectively, these findings strongly suggest that an important proportion of Ly-6C$^-$CD44^{hi} γδ T lymphocytes corresponds to long-term SLO-resident cells in the steady state.

Macrophages are responsible for the long-term trapping of Ly-6C$^-$CD44^{hi} γδ T lymphocytes within SLOs in the steady state

We then attempted to identify the cellular actors involved in the retention of Ly-6C$^-$CD44^{hi} γδ T cells within SLOs. We first studied the potential involvement of B cells in this process. B cell–deficient or –proficient C57BL/6 mice were treated or not with integrin-neutralizing Abs and analyzed 48 h later (Fig. 3A). The retention rate (recovery) of Ly-6C$^-$CD44^{hi} γδ T cells in pLNs and mLNs was comparable in both mouse strains, 48 h after blocking T cell entry (Fig. 3B). Thus, B lymphocytes do not seem to be involved in the trapping of Ly-6C$^-$CD44^{hi} γδ T cells within LNs.

We next assessed whether DCs played a role in the retention of this γδ T cell subset in LNs. For this purpose, C57BL/6 CD11c.DTR mice (designated CD11c.DOG), which allow, following DT injections, a continuous in vivo depletion of DCs, were injected or not with anti–LFA-1 and anti–VLA-4 Abs (Fig. 3C). We first assessed the depletion efficiency of such a protocol (Supplemental Fig. 2A, 2B). Depletion was quite efficient for plasmacytoid DCs in all LNs and better for the other DC subsets in mLNs than in pLNs. The recovery of Ly-6C$^-$CD44^{hi} γδ T cells in both pLNs and mLNs 48 h after blocking T cell entry into LNs was not diminished by DC depletion (Fig. 3D), suggesting that these latter cells are not crucially involved in the retention of Ly-6C$^-$CD44^{hi} γδ T cells within SLOs.

Finally, we examined whether macrophages could contribute to Ly-6C$^-$CD44^{hi} γδ T cell retention within SLOs. To test this hypothesis, C57BL/6 mice were fed with mouse chow containing an inhibitor of CSF1R (PLX3397; provided by Plexxikon) for 7 d (Fig. 3E). We first assessed the depletion efficiency of such a protocol (Supplemental Fig. 1C). This protocol led to the depletion of most subcapsular (F4/80$^-$ CD169$^+$) and medullary (F4/80$^+$ CD169$^+$) sinus macrophages in both pLNs and mLNs, whereas F4/80$^+$CD169$^-$ macrophages were only poorly affected, especially

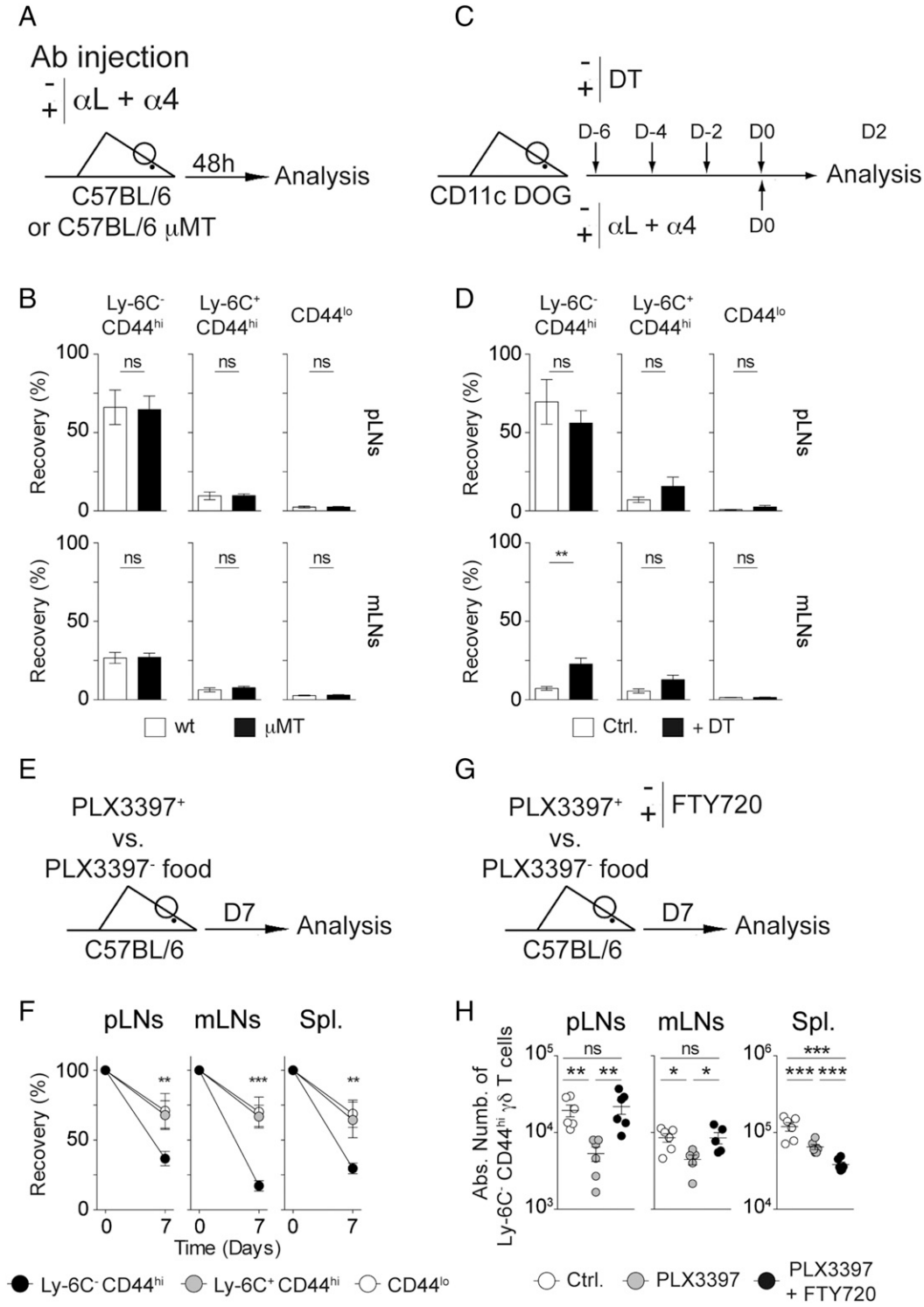

FIGURE 3. Macrophages are responsible for the long-term trapping of Ly-6C$^-$CD44^{hi} γδ T lymphocytes within SLOs in the steady state. (**A** and **B**) C57BL/6 and C57BL/6 μMT mice were treated or not with integrin-neutralizing Abs and analyzed 48 h later. (A) Diagram illustrating the experimental model. (B) Percentage of γδ T cell subset recovery (calculated as in Fig. 1D) within pLNs and mLNs of anti–LFA-1– and anti-VLA-4–treated C57BL/6 and C57BL/6 μMT mice. (**C** and **D**) C57BL/6 CD11c.DTR mice (designated CD11c.DOG) were injected or not with integrin-neutralizing Abs and DT. (C) Diagram illustrating the experimental model. (D) Percentage of γδ T cell subset recovery within pLNs and mLNs of anti–LFA-1– and anti-VLA-4–treated control and DT-injected mice. (**E** and **F**) C57BL/6 mice were fed with mouse chow containing or not an inhibitor of CSF1R (PLX3397). Seven days after PLX3397 feeding, pLNs, mLNs, and spleen were recovered separately. (E) Diagram illustrating the experimental model. (F) Percentage of γδ T cell subset recovery within pLNs, mLNs, and spleen of PLX3397 fed mice. (**G** and **H**) C57BL/6 mice were fed with mouse chow containing or not PLX3397 and daily injected or not with FTY720. Seven days after PLX3397 and FTY treatments, pLNs, mLNs, and spleen were recovered separately. (G) Diagram illustrating the experimental model. (H) Absolute numbers of Ly-6C$^-$CD44^{hi} γδ T cells recovered from pLNs, mLNs, and spleen of control (Ctrl.), PLX3397-, and PLX3397 plus FTY720–treated mice. For (B), (D), (F), and (H), results are shown as mean ± SEM for at least three mice per group per experiment, from at least two independent experiments. $*p < 0.05$, $**p < 0.01$, $***p < 0.001$. α4, anti–VLA-4; Ctrl., control; αL, anti–LFA-1; Spl., spleen.

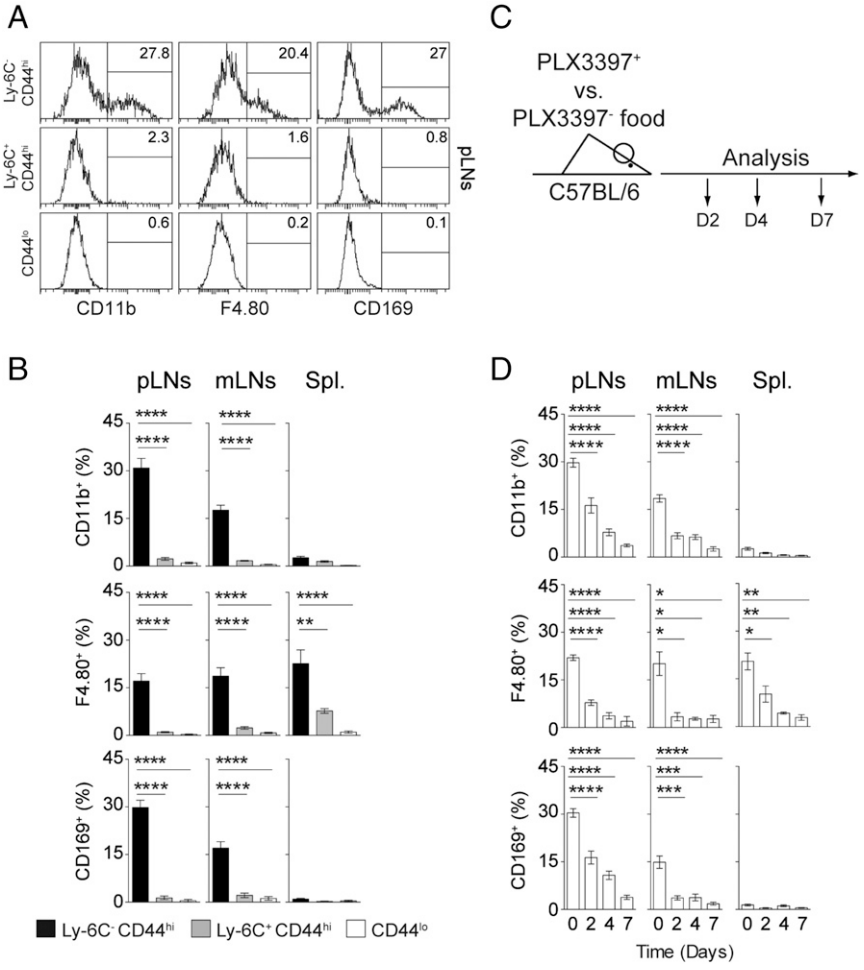

FIGURE 4. Membrane blebs reveal the close intimacy between Ly-6C$^-$CD44^{hi} γδ T lymphocytes and macrophage subsets in SLOs. (**A**) CD11b, F4/80, and CD169 fluorescence histograms of γδ T cell subsets recovered from pLNs are shown for a representative C57BL/6 mouse. Numbers in each histogram represent the percentage of CD11b$^+$ F4/80$^+$, or CD169$^+$ cells among γδ T cell subsets. (**B**) The proportions of CD11b$^+$, F4/80$^+$, or CD169$^+$ cells among γδ T cell subsets recovered from pLNs, mLNs, and spleen of C57BL/6 mice were calculated. (**C** and **D**) C57BL/6 mice were fed with mouse chow containing or not an inhibitor of CSF1R (PLX3397). Two, 4, and 7 days after PLX3397 feeding, pLNs, mLNs, and spleen were recovered separately. (C) Diagram illustrating the experimental model. (D) The proportions of CD11b$^+$, F4/80$^+$, or CD169$^+$ cells among Ly-6C$^-$CD44^{hi} γδ T cells recovered from pLNs, mLNs, and spleen of C57BL/6 mice were calculated. Results are shown as mean ± SEM for at least three mice per group per experiment, from at least three independent experiments. $*p < 0.05$, $**p < 0.01$, $***p < 0.001$, $****p < 0.0001$. Spl., spleen.

in pLNs. We found that the absolute numbers of Ly-6C$^-$CD44^{hi} γδ T cells in pLNs, mLNs, and the spleen dropped dramatically in mice fed 7 d with PLX3397 chow (Fig. 3F). Although the absolute numbers of the other γδ T cell subsets were also affected, the observed decreases were far less pronounced (Fig. 3F).

We hypothesized that macrophages would be required for Ly-6C$^-$CD44^{hi} γδ T cell retention within SLOs. In such a model, macrophage depletion would lead to the egress of Ly-6C$^-$CD44^{hi} γδ T cells from SLOs and that would account for the significant drop in absolute numbers observed in mice treated 7 d with PLX3397. The membrane receptor S1PR1, by allowing T cells to respond to the sphingolipid S1P present within efferent lymph, is the central mediator of lymphocyte egress from SLOs (31, 32). First, we studied S1PR1 expression by γδ T cell subsets recovered from pLNs, mLNs, and the spleen (Supplemental Fig. 3). We found that Ly-6C$^-$CD44^{hi} γδ T cells from pLNs and mLNs exhibited higher S1PR1 surface levels than did the other γδ T cell subsets. Ly-6C$^-$CD44^{hi} γδ T cells should be thus highly sensitive to S1P gradients. Then, C57BL/6 mice were fed with PLX3397 chow and daily injected or not for 7 d with FTY720 (Fig. 3G). Interestingly, FTY720 injections fully abrogated the strong decrease in Ly-6C$^-$CD44^{hi} γδ T cell absolute numbers provoked by the PLX3397 treatment in both pLNs and mLNs (Fig. 3H). These results suggest that CSF1R inhibitor administration is not toxic to γδ T cells but rather allows them to egress from LNs through an S1PR1-dependent mechanism. Of note, FTY720 administration did not abolish the effect of the PLX3397 treatment in the spleen but rather accentuated the observed decrease of the absolute number of Ly-6C$^-$CD44^{hi} γδ T cells (Fig. 3G). This result could be explained by the duration of the S1PR1 agonist treatment. More precisely, it has already been described that whereas a single injection of FTY720 induces T cell sequestration in the spleen (33, 34), a prolonged FTY720 treatment rather leads, in this SLO, to a decrease in the absolute numbers of T lymphocytes (34–36).

Taken together, these last results suggest that macrophages play a crucial role in the long-term trapping of Ly-6C$^-$CD44^{hi} γδ T lymphocytes within SLOs.

Membrane blebs reveal the close intimacy between Ly-6C$^-$CD44^{hi} γδ T lymphocytes and macrophages in SLOs

It has recently been shown that an important fraction of IL-17–committed T lymphocytes from pLNs could acquire membrane blebs from subcapsular sinus macrophages, reflecting the intimacy of the crosstalk between these two cell types (37). We thus examined the proportion of Ly-6C$^-$CD44^{hi}, Ly-6C$^+$CD44^{hi}, and Ly-6C$^+$CD44^{lo} γδ T lymphocytes expressing macrophage markers such as CD11b, F4/80, and CD169 (Fig. 4A, 4B). Expression of these three molecules was solely detected on the cell surface of Ly-6C$^-$CD44^{hi} γδ T cells. Interestingly, the surface expression of CD11b, F4/80, and CD169 by Ly-6C$^-$CD44^{hi} γδ T lymphocytes seemed to vary depending on the location of these cells (pLNs versus mLNs versus the spleen; Fig. 4B), suggesting the ability of Ly-6C$^-$CD44^{hi} γδ T lymphocytes to initiate intimate crosstalk with various macrophage subsets such as subcapsular sinus macrophages (CD11b$^+$F4/80$^-$CD169$^+$), medullary sinus macrophages (CD11b$^+$F4/80$^+$CD169$^+$), or spleen red pulp macrophages (CD11b$^-$F4/80$^+$CD169$^-$) (38–40). More precisely, the observed

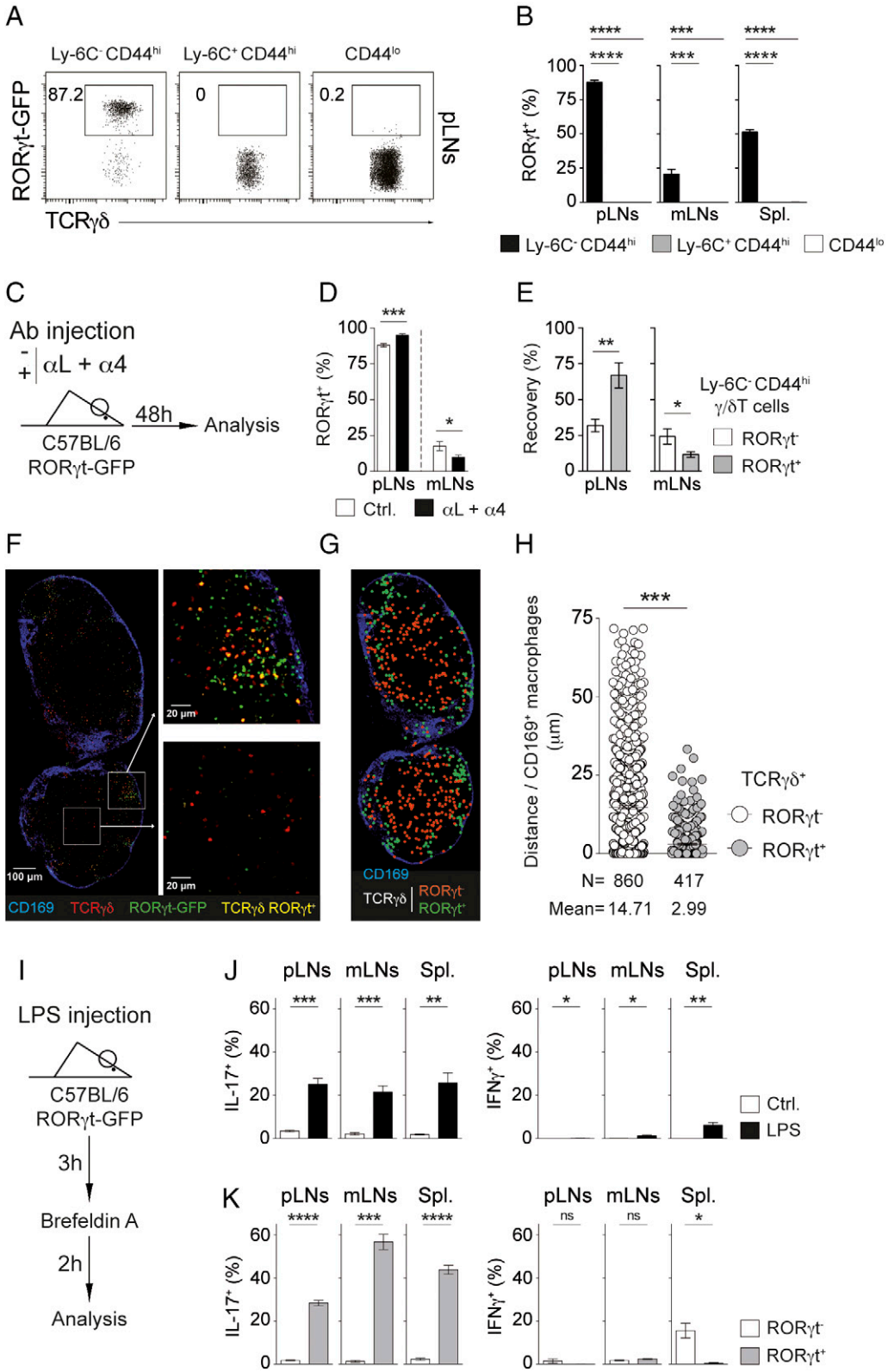

FIGURE 5. RORγt expression allows determination of the location of resident γδ T cells within pLNs. (**A**) RORγt/TCRγδ dot plots for gated γδ T cell subsets recovered from pLNs of a representative C57BL/6 RORγt-GFP mouse. (**B**) The proportions of RORγt$^+$ cells among γδ T cell subsets recovered from pLNs, mLNs, and spleen of C57BL/6 RORγt-GFP mice were calculated. (**C**–**E**) C57BL/6 RORγt-GFP mice have been injected i.p. with integrin-neutralizing anti–LFA-1 and anti–VLA-4 Abs. Two days after treatment, pLNs and mLNs were recovered separately. (C) Diagram illustrating the experimental model. (D) The proportions of RORγt$^+$ cells among Ly-6C$^-$CD44^{hi} γδ T cells recovered from pLNs and mLNs of treated or untreated mice were calculated. (E) Percentage of RORγt$^+$ and RORγt$^-$ Ly-6C$^-$CD44^{hi} γδ T cell recovery (calculated as in Fig. 1) within pLNs and mLNs of anti–LFA-1– and anti-VLA-4–treated mice. Results are shown as mean ± SEM for at least three mice per group per experiment, from at least three independent experiments. (**F**–**H**) Location of RORγt$^-$ and RORγt$^+$ γδ T cells within pLNs from C57BL/6 RORγt-GFP mice was examined. (F) Representative immunofluorescence TCRγδ, CD169, and RORγt-GFP staining of fixed pLNs slices (maxillary LN is shown here). RORγt$^+$ γδ T cells appear in (*Figure legend continues*)

proportions of Ly-6C$^-$CD44^{hi} γδ T cells acquiring CD11b, F4/80, and CD169 expression suggest that these cells interact preferentially with subcapsular and medullary sinus macrophages within pLNs (30% of Ly-6C$^-$CD44^{hi} γδ T cells from pLNs expressed CD11b and CD169 whereas only 15% expressed F4/80), with medullary sinus macrophages in mLNs [equal proportions (15%) of cells from mLNs expressing CD11b, F4/80, and CD169] and with red pulp macrophages in the spleen (Ly-6C$^-$CD44^{hi} γδ T cells only expressed F4/80) (Fig. 4B, Supplemental Fig. 4).

Using the PLX3397$^+$ feeding strategy, we then studied the consequences of macrophage depletion on the expression of macrophage markers by Ly-6C$^-$CD44^{hi} γδ T lymphocytes (Fig. 4C). Following PLX3397 treatment, there was a gradual decrease with time in the proportion of SLO Ly-6C$^-$CD44^{hi} γδ T cells expressing CD11b, F4/80, or CD169 (Fig. 4D). These latter results confirm that the expression of CD11b, F4/80, and CD169 by this γδ T cell subset results from the transfer of membrane blebs from macrophages to γδ T cells.

Collectively, our results suggest that Ly-6C$^-$CD44^{hi} γδ T lymphocytes initiate strong adhesive interactions with macrophages that may lead to their long-term retention within SLOs.

RORγt expression allows determination of the localization of resident γδ T cells within pLNs

We have described above a clear enrichment in IL-17–producing cells among γδ T cells in LNs, 48 h after blocking T cell entry into these SLOs (Fig. 1E, 1F). We thus hypothesized that the expression of the transcription factor RORγt may allow a precise identification of resident γδ T cells in SLOs. We first evaluated the proportion of Ly-6C$^-$CD44^{hi}, Ly-6C$^+$CD44^{hi}, and Ly-6C$^+$CD44^{lo} γδ T lymphocytes expressing RORγt in SLOs by using RORγt-GFP transgenic mice (Fig. 5A, 5B). In agreement with the fact that only Ly-6C$^-$CD44^{hi} γδ T lymphocytes are able to produce IL-17 (15), we found that RORγt expression was restricted to these cells. Surprisingly, the proportion of RORγt$^+$ cells within Ly-6C$^-$CD44^{hi} γδ T cells differed considerably depending on the organ studied. Indeed, whereas the vast majority (~80%) of Ly-6C$^-$CD44^{hi} γδ T lymphocytes recovered from pLNs expressed RORγt, this proportion was quite lower in mLNs and the spleen (Fig. 5B). We then examined the expression of RORγt by LN-resident γδ T lymphocytes 48 h after blocking T cell entry (Fig. 5C–E). In pLNs, after treatment, the proportion of Ly-6C$^-$CD44^{hi} γδ T cells expressing RORγt was significantly higher than in pLNs from control mice (Fig. 5D). Accordingly, 48 h after blocking T cell entry, the recovery of RORγt$^+$Ly-6C$^-$CD44^{hi} γδ T cells was far better than the recovery observed for their RORγt$^-$ cell counterparts (Fig. 5E). This was not the case for mLNs, as in this SLO, RORγt$^-$Ly-6C$^-$CD44^{hi} γδ T cells were more efficiently retained after treatment than RORγt$^+$Ly-6C$^-$CD44^{hi} γδ T cells (Fig. 5D, 5E).

Altogether, these results suggest that the expression of RORγt can be considered as a reliable marker to identify resident γδ T cells within pLNs (but not in mLNs). Thus, to study the location of resident γδ T cells in pLNs, we imaged pLN slices recovered from RORγt-GFP mice by immunofluorescence microscopy (Fig. 5F–H). In line with the capacity of Ly-6C$^-$CD44^{hi} γδ T lymphocytes to acquire membrane blebs from subcapsular and medullary sinus macrophages, we clearly observed that RORγt$^+$ γδ T cells (most of which are resident cells within pLNs) were localized close to CD169$^+$ sinus macrophages (Fig. 5F, 5G). Quantification of the distance between RORγt$^-$ or RORγt$^+$ γδ T cells and CD169$^+$ cells confirmed that RORγt$^+$ γδ T cells were very significantly far closer to CD169$^+$ cells than their RORγt$^-$ cell counterparts (Fig. 5H). Such a close vicinity may help explain the capacity of Ly-6C$^-$CD44^{hi} γδ T cells to acquire macrophage-related surface markers, and such interactions may lead to the long-term retention of these cells within SLOs.

Ly-6C$^-$CD44^{hi} γδ T lymphocytes from SLOs respond rapidly in vivo to LPS challenge

As described above, our results suggest that Ly-6C$^-$CD44^{hi} γδ T lymphocytes initiate strong adhesive interactions with macrophages that may lead to their long-term retention within SLOs. Additionally, we observed that resident RORγt$^+$ γδ T cells were localized close to CD169$^+$ sinus macrophages within pLNs. We thus hypothesized that SLO-resident γδ T cells could represent sentinels surveying the pathogen-exposed surface of SLOs.

To address this issue, RORγt-GFP transgenic mice were injected i.v. with LPS. IL-17 and IFN-γ productions by Ly-6C$^-$CD44^{hi} γδ T cells recovered from pLNs, mLNs, and the spleen were then analyzed 3 h later (Fig. 5I). We observed that, in all SLOs, ~20% of Ly-6C$^-$CD44^{hi} γδ T cells were already producing IL-17 in response to LPS challenge at this early time point (Fig. 5J). Additionally, we noticed that IL-17 production was restricted to RORγt-expressing cells (Fig. 5K). Of note, in the same setting, we detected a small proportion of IFN-γ–producing Ly-6C$^-$CD44^{hi} γδ T cells in the spleen, and this IFN-γ production was restricted to RORγt$^-$ cells (Fig. 5J, 5K). The capacity of Ly-6C$^-$CD44^{hi} γδ T cells to rapidly produce IL-17 upon LPS challenge strongly suggests that these SLO-resident γδ T cells could play a crucial surveying role to protect these organs from infections.

Discussion

To achieve their surveying task for foreign Ags and survival signals, peripheral T cells have been described as having a nomadic existence between blood, SLOs, and lymph in the steady state (16, 17). Transit times within SLOs should be 1) not too long, as T cells must continuously scan APCs from different LNs to find where the next pathogen will cross the epithelial barrier, but also 2) not too rapid to avoid missing the rare APCs presenting their specific Ag in SLOs in the early phases of an infection. However, in parallel to that model, recent findings highlight the existence of T cells residing for long periods of time within nonlymphoid tissues (41). More precisely, subsets of CD8$^+$ and CD4$^+$ αβ T cells but also subsets of NK cells, NKT cells, and γδ T cells have been shown to reside within nonlymphoid tissues such as the skin, gut, lungs, or adipose tissue, providing rapid and efficient protection

yellow. Squares indicate zoomed areas presented on the figure. (G) Location modeling of RORγt$^-$ and RORγt$^+$ γδ T lymphocytes within pLNs (maxillary LN is shown here). Coordinates of all RORγt$^-$ and RORγt$^+$ γδ T cells were calculated from immunofluorescence staining shown in (F) and were then reapplied on CD169-stained LN slice. (H) Distance between RORγt$^-$ and RORγt$^+$ γδ T lymphocytes and CD169$^+$ cells were calculated. (**I–K**) C57BL/6 RORγt-GFP mice were injected i.v. with LPS. Three hours later, cells recovered from pLNs, mLNs, and spleen were incubated during 2 h with brefeldin A for determination of intracellular cytokine production. (I) Diagram illustrating the experimental model. (J) Percentage of IL-17– and IFN-γ–producing cells among Ly-6C$^-$CD44^{hi} γδ T cells recovered from pLNs, mLNs, and spleen of control and LPS-treated mice. (K) Percentage of IL-17– and IFN-γ–producing cells among RORγt$^-$ and RORγt$^+$ Ly-6C$^-$CD44^{hi} γδ T cells recovered from pLNs, mLNs, and spleen of LPS-treated mice. Results are shown as mean ± SEM for at least three different LN slices from three different mice. *$p < 0.05$, **$p < 0.01$, ***$p < 0.001$, ****$p < 0.0001$. α4, anti–VLA-4; Ctrl., control; αL, anti–LFA-1; Spl., spleen.

against reinfection by tissue-tropic pathogens but also promoting the repair of damaged tissues (42–47).

In the present study, using injection of integrin-neutralizing Abs and parabiosis strategies, we highlight the existence of γδ T cells residing in the steady state in the SLOs of specific pathogen-free mice. In line with our results, Zhang et al. (32) have recently shown that innate-like T cells defined as expressing high surface levels of CD127 and CCR6, among which about one fourth corresponds to γδ T cells, accumulated near the subcapsular sinus in pLNs. In this study, we confirm and extend these observations. First, whereas Zhang et al. (32) examined the amount of cell exchange 2 wk after surgery in parabiotic mice or 2 d after T cell photoconversion in photoconvertible fluorescence protein Kaede transgenic mice, our parabiosis experiments clearly showed that full chimerism between the two parabionts was still not reached in pLNs for Ly-6C$^-$CD44^{hi} γδ T cells at least up to 2 mo after surgery (Fig. 2). Thus, in this study we demonstrate the long-term residency of these cells within pLNs. Second, we showed that the long-term retention of Ly-6C$^-$CD44^{hi} γδ T cells was not a peculiar feature of pLNs, as it also applies to mLNs and the spleen. Third, although we confirmed that in pLNs, innate-like Ly-6C$^-$CD44^{hi} γδ T lymphocytes were located close to subcapsular sinus macrophages and were able to acquire, from this vicinity, the apparent expression of CD11b and CD169, our results strongly suggest that other subsets of macrophages are involved in the retention of these cells within SLOs (see below). Finally, we have also studied the behavior of the other γδ T cell subsets (i.e., Ly-6C$^+$CD44^{hi} and Ly-6C$^{-/+}$CD44^{lo} γδ T cells) in SLOs and showed that whatever their naive-like or memory-like phenotype, they corresponded to circulating cells.

In addition to the CD11b and CD169 markers, about half of CD11b-expressing innate-like γδ T cells in pLNs and all of them in mLNs were also acquiring F4/80 expression (Fig. 4B). Similar to CD11b and CD169, F4/80 surface expression by γδ T cells decreased gradually following in vivo macrophage depletion, suggesting that innate-like γδ T cells are not only interacting with subcapsular (CD11b$^+$F4/80$^-$CD169$^+$) sinus macrophages but also with medullary (CD11b$^+$F4/80$^+$CD169$^+$) sinus macrophages. Finally, our parabiosis experiments show that a fraction of Ly-6C$^-$CD44^{hi} γδ T cells are also residing for long periods of time in the spleen. In this SLO, only F4/80 was detected at the cell surface of Ly-6C$^-$CD44^{hi} γδ T cells. This latter result suggests that resident γδ T lymphocytes are interacting with splenic red pulp (CD11b$^-$F4/80$^+$CD169$^-$) macrophages. Such a hypothesis would be in agreement with previous studies that have observed a preferential localization of human and mice γδ T lymphocytes within the red pulp of the spleen (48, 49). Interactions between tissue-resident γδ T cells and F4/80$^+$ macrophages have been reported in the lungs in mice (50). Indeed, it has been shown that pulmonary-resident γδ T cells had an intrinsic preference to interact with F4/80$^+$ macrophages (51). These continuous interactions would be important for their protective role as sentinels of airways and lung tissues.

Collectively, our data suggest that the precise nature of resident γδ T cells but also of the macrophages involved in their retention varies according to the SLOs analyzed (pLNs versus mLNs versus the spleen). Indeed, whereas in pLNs, the residence of Ly-6C$^-$CD44^{hi} γδ T cells was mostly restricted to RORγt$^+$ cells, RORγt$^-$ cells were more efficiently trapped in mLNs than their RORγt$^+$ cell counterparts. Furthermore, whereas both subcapsular and medullary sinus macrophages would be involved in the retention of Ly-6C$^-$CD44^{hi} γδ T cells in pLNs, the role of subcapsular sinus macrophages would be less crucial in mLNs and the spleen. Indeed, medullary sinus and red pulp macrophages appear as the main actors implied in the retention of γδ T cells in mLNs and the spleen, respectively. Sinus and red pulp macrophages have a propensity to capture particulate material arriving in the lymph and the blood (52–54). Thus, we hypothesize that resident Ly-6C$^-$CD44^{hi} γδ T cells could play a critical surveillance role in protecting SLOs from infections. In our previous study, we showed that Ly-6C$^-$CD44^{hi} γδ T cells possessed innate-like properties such as the ability to respond directly to TLR ligands in vitro (15). In this study, we found that Ly-6C$^-$CD44^{hi} γδ T cells from SLOs were rapidly able to produce IL-17 in vivo in response to LPS challenge. In this setting, LPS may activate them directly or indirectly through the induction of IL-23 and IL-1β production by neighboring macrophages, as it has been described that RORγt$^+$ γδ T cells express IL-23R and produce IL-17 in response to IL-1β and IL-23, without TCR engagement (6). We are thus proposing that resident γδ T cells and macrophages could have complementary roles and may represent a major barrier blocking the systemic spread of pathogens within SLOs by providing rapid innate responses.

Acknowledgments

We are grateful to Plexxikon for providing the PLX3397 inhibitor. We thank the Cochin Cytometry and Immunobiology (CIBIO), Cochin Imaging Photonic (IMAG'IC), and Cochin Animal Core facilities for their technological support.

Disclosures

The authors have no financial conflicts of interest.

References

1. Chien, Y. H., C. Meyer, and M. Bonneville. 2014. γδ T cells: first line of defense and beyond. *Annu. Rev. Immunol.* 32: 121–155.
2. Nanno, M., Y. Kanari, T. Naito, N. Inoue, T. Hisamatsu, H. Chinen, K. Sugimoto, Y. Shimomura, H. Yamagishi, T. Shiohara, et al. 2008. Exacerbating role of γδ T cells in chronic colitis of T-cell receptor α mutant mice. *Gastroenterology* 134: 481–490.
3. Mombaerts, P., E. Mizoguchi, M. J. Grusby, L. H. Glimcher, A. K. Bhan, and S. Tonegawa. 1993. Spontaneous development of inflammatory bowel disease in T cell receptor mutant mice. *Cell* 75: 274–282.
4. Roark, C. L., J. D. French, M. A. Taylor, A. M. Bendele, W. K. Born, and R. L. O'Brien. 2007. Exacerbation of collagen-induced arthritis by oligoclonal, IL-17-producing γδ T cells. *J. Immunol.* 179: 5576–5583.
5. Keystone, E. C., C. Rittershaus, N. Wood, K. M. Snow, J. Flatow, J. C. Purvis, L. Poplonski, and P. C. Kung. 1991. Elevation of a γδ T cell subset in peripheral blood and synovial fluid of patients with rheumatoid arthritis. *Clin. Exp. Immunol.* 84: 78–82.
6. Sutton, C. E., S. J. Lalor, C. M. Sweeney, C. F. Brereton, E. C. Lavelle, and K. H. Mills. 2009. Interleukin-1 and IL-23 induce innate IL-17 production from γδ T cells, amplifying Th17 responses and autoimmunity. *Immunity* 31: 331–341.
7. Wucherpfennig, K. W., P. Höllsberg, J. H. Richardson, D. Benjamin, and D. A. Hafler. 1992. T-cell activation by autologous human T-cell leukemia virus type I-infected T-cell clones. *Proc. Natl. Acad. Sci. USA* 89: 2110–2114.
8. Street, S. E., Y. Hayakawa, Y. Zhan, A. M. Lew, D. MacGregor, A. M. Jamieson, A. Diefenbach, H. Yagita, D. I. Godfrey, and M. J. Smyth. 2004. Innate immune surveillance of spontaneous B cell lymphomas by natural killer cells and γδ T cells. *J. Exp. Med.* 199: 879–884.
9. Girardi, M., D. E. Oppenheim, C. R. Steele, J. M. Lewis, E. Glusac, R. Filler, P. Hobby, B. Sutton, R. E. Tigelaar, and A. C. Hayday. 2001. Regulation of cutaneous malignancy by γδ T cells. *Science* 294: 605–609.
10. Liu, Z., I. E. Eltoum, B. Guo, B. H. Beck, G. A. Cloud, and R. D. Lopez. 2008. Protective immunosurveillance and therapeutic antitumor activity of γδ T cells demonstrated in a mouse model of prostate cancer. *J. Immunol.* 180: 6044–6053.
11. Gao, Y., W. Yang, M. Pan, E. Scully, M. Girardi, L. H. Augenlicht, J. Craft, and Z. Yin. 2003. γδ T cells provide an early source of interferon γ in tumor immunity. *J. Exp. Med.* 198: 433–442.
12. Lança, T., M. F. Costa, N. Gonçalves-Sousa, M. Rei, A. R. Grosso, C. Penido, and B. Silva-Santos. 2013. Protective role of the inflammatory CCR2/CCL2 chemokine pathway through recruitment of type 1 cytotoxic γδ T lymphocytes to tumor beds. *J. Immunol.* 190: 6673–6680.
13. Lafont, V., F. Sanchez, E. Laprevotte, H. A. Michaud, L. Gros, J. F. Eliaou, and N. Bonnefoy. 2014. Plasticity of γδ T cells: impact on the anti-tumor response. *Front. Immunol.* 5: 622.
14. Coffelt, S. B., K. Kersten, C. W. Doornebal, J. Weiden, K. Vrijland, C. S. Hau, N. J. Verstegen, M. Ciampricotti, L. J. Hawinkels, J. Jonkers, and K. E. de Visser. 2015. IL-17-producing γδ T cells and neutrophils conspire to promote breast cancer metastasis. *Nature* 522: 345–348.
15. Lombes, A., A. Durand, C. Charvet, M. Rivière, N. Bonilla, C. Auffray, B. Lucas, and B. Martin. 2015. Adaptive immune-like γ/δ T lymphocytes share

many common features with their α/β T cell counterparts. *J. Immunol.* 195: 1449–1458.
16. von Andrian, U. H., and T. R. Mempel. 2003. Homing and cellular traffic in lymph nodes. *Nat. Rev. Immunol.* 3: 867–878.
17. Gowans, J. L., and E. J. Knight. 1964. The route of re-circulation of lymphocytes in the rat. *Proc. R. Soc. Lond. B Biol. Sci.* 159: 257–282.
18. Mandl, J. N., R. Liou, F. Klauschen, N. Vrisekoop, J. P. Monteiro, A. J. Yates, A. Y. Huang, and R. N. Germain. 2012. Quantification of lymph node transit times reveals differences in antigen surveillance strategies of naive $CD4^+$ and $CD8^+$ T cells. *Proc. Natl. Acad. Sci. USA* 109: 18036–18041.
19. Vantourout, P., and A. Hayday. 2013. Six-of-the-best: unique contributions of γδ T cells to immunology. *Nat. Rev. Immunol.* 13: 88–100.
20. Silva-Santos, B., K. Serre, and H. Norell. 2015. γδ T cells in cancer. *Nat. Rev. Immunol.* 15: 683–691.
21. Akitsu, A., H. Ishigame, S. Kakuta, S. H. Chung, S. Ikeda, K. Shimizu, S. Kubo, Y. Liu, M. Umemura, G. Matsuzaki, et al. 2015. IL-1 receptor antagonist-deficient mice develop autoimmune arthritis due to intrinsic activation of IL-17-producing $CCR2^+V\gamma6^+\gamma\delta$ T cells. *Nat. Commun.* 6: 7464.
22. Ramírez-Valle, F., E. E. Gray, and J. G. Cyster. 2015. Inflammation induces dermal $V\gamma4^+$ γδT17 memory-like cells that travel to distant skin and accelerate secondary IL-17–driven responses. *Proc. Natl. Acad. Sci. USA* 112: 8046–8051.
23. Penido, C., M. F. Costa, M. C. Souza, K. A. Costa, A. L. Candéa, C. F. Benjamim, and Md. Henriques. 2008. Involvement of CC chemokines in γδ T lymphocyte trafficking during allergic inflammation: the role of CCL2/CCR2 pathway. *Int. Immunol.* 20: 129–139.
24. Hochweller, K., J. Striegler, G. J. Hämmerling, and N. Garbi. 2008. A novel CD11c.DTR transgenic mouse for depletion of dendritic cells reveals their requirement for homeostatic proliferation of natural killer cells. *Eur. J. Immunol.* 38: 2776–2783.
25. Lochner, M., L. Peduto, M. Cherrier, S. Sawa, F. Langa, R. Varona, D. Riethmacher, M. Si-Tahar, J. P. Di Santo, and G. Eberl. 2008. In vivo equilibrium of proinflammatory $IL\text{-}17^+$ and regulatory $IL\text{-}10^+$ $Foxp3^+$ $ROR\gamma t^+$ T cells. *J. Exp. Med.* 205: 1381–1393.
26. Le Campion, A., A. Pommier, A. Delpoux, L. Stouvenel, C. Auffray, B. Martin, and B. Lucas. 2012. IL-2 and IL-7 determine the homeostatic balance between the regulatory and conventional $CD4^+$ T cell compartments during peripheral T cell reconstitution. *J. Immunol.* 189: 3339–3346.
27. Pommier, A., A. Audemard, A. Durand, R. Lengagne, A. Delpoux, B. Martin, L. Douguet, A. Le Campion, M. Kato, M. F. Avril, et al. 2013. Inflammatory monocytes are potent antitumor effectors controlled by regulatory $CD4^+$ T cells. *Proc. Natl. Acad. Sci. USA* 110: 13085–13090.
28. Delpoux, A., P. Yakonowsky, A. Durand, C. Charvet, M. Valente, A. Pommier, N. Bonilla, B. Martin, C. Auffray, and B. Lucas. 2014. TCR signaling events are required for maintaining CD4 regulatory T cell numbers and suppressive capacities in the periphery. *J. Immunol.* 193: 5914–5923.
29. Martin, B., C. Auffray, A. Delpoux, A. Pommier, A. Durand, C. Charvet, P. Yakonowsky, H. de Boysson, N. Bonilla, A. Audemard, et al. 2013. Highly self-reactive naive CD4 T cells are prone to differentiate into regulatory T cells. *Nat. Commun.* 4: 2209.
30. Narayan, K., K. E. Sylvia, N. Malhotra, C. C. Yin, G. Martens, T. Vallerskog, H. Kornfeld, N. Xiong, N. R. Cohen, M. B. Brenner, et al; Immunological Genome Project Consortium. 2012. Intrathymic programming of effector fates in three molecularly distinct γδ T cell subtypes. *Nat. Immunol.* 13: 511–518.
31. Cyster, J. G., and S. R. Schwab. 2012. Sphingosine-1-phosphate and lymphocyte egress from lymphoid organs. *Annu. Rev. Immunol.* 30: 69–94.
32. Zhang, Y., T. L. Roth, E. E. Gray, H. Chen, L. B. Rodda, Y. Liang, P. Ventura, S. Villeda, P. R. Crocker, and J. G. Cyster. 2016. Migratory and adhesive cues controlling innate-like lymphocyte surveillance of the pathogen-exposed surface of the lymph node. *eLife* 5: e18156.
33. Mandala, S., R. Hajdu, J. Bergstrom, E. Quackenbush, J. Xie, J. Milligan, R. Thornton, G. J. Shei, D. Card, C. Keohane, et al. 2002. Alteration of lymphocyte trafficking by sphingosine-1-phosphate receptor agonists. *Science* 296: 346–349.
34. Morris, M. A., D. R. Gibb, F. Picard, V. Brinkmann, M. Straume, and K. Ley. 2005. Transient T cell accumulation in lymph nodes and sustained lymphopenia in mice treated with FTY720. *Eur. J. Immunol.* 35: 3570–3580.
35. Hofmann, M., V. Brinkmann, and H. G. Zerwes. 2006. FTY720 preferentially depletes naive T cells from peripheral and lymphoid organs. *Int. Immunopharmacol.* 6: 1902–1910.
36. Schwab, S. R., and J. G. Cyster. 2007. Finding a way out: lymphocyte egress from lymphoid organs. *Nat. Immunol.* 8: 1295–1301.
37. Gray, E. E., S. Friend, K. Suzuki, T. G. Phan, and J. G. Cyster. 2012. Subcapsular sinus macrophage fragmentation and $CD169^+$ bleb acquisition by closely associated IL-17-committed innate-like lymphocytes. *PLoS One* 7: e38258.
38. Gray, E. E., and J. G. Cyster. 2012. Lymph node macrophages. *J. Innate Immun.* 4: 424–436.
39. Franken, L., M. Schiwon, and C. Kurts. 2016. Macrophages: sentinels and regulators of the immune system. *Cell. Microbiol.* 18: 475–487.
40. Franken, L., M. Klein, M. Spasova, A. Elsukova, U. Wiedwald, M. Welz, P. Knolle, M. Farle, A. Limmer, and C. Kurts. 2015. Splenic red pulp macrophages are intrinsically superparamagnetic and contaminate magnetic cell isolates. *Sci. Rep.* 5: 12940.
41. Mueller, S. N., and L. K. Mackay. 2016. Tissue-resident memory T cells: local specialists in immune defence. *Nat. Rev. Immunol.* 16: 79–89.
42. Turner, D. L., and D. L. Farber. 2014. Mucosal resident memory CD4 T cells in protection and immunopathology. *Front. Immunol.* 5: 331.
43. Panduro, M., C. Benoist, and D. Mathis. 2016. Tissue Tregs. *Annu. Rev. Immunol.* 34: 609–633.
44. Peng, H., X. Jiang, Y. Chen, D. K. Sojka, H. Wei, X. Gao, R. Sun, W. M. Yokoyama, and Z. Tian. 2013. Liver-resident NK cells confer adaptive immunity in skin-contact inflammation. *J. Clin. Invest.* 123: 1444–1456.
45. Lynch, L., X. Michelet, S. Zhang, P. J. Brennan, A. Moseman, C. Lester, G. Besra, E. E. Vomhof-Dekrey, M. Tighe, H. F. Koay, et al. 2015. Regulatory *i*NKT cells lack expression of the transcription factor PLZF and control the homeostasis of T_{reg} cells and macrophages in adipose tissue. *Nat. Immunol.* 16: 85–95.
46. Di Marco Barros, R., N. A. Roberts, R. J. Dart, P. Vantourout, A. Jandke, O. Nussbaumer, L. Deban, S. Cipolat, R. Hart, M. L. Iannitto, et al. 2016. Epithelia use butyrophilin-like molecules to shape organ-specific γδ T cell compartments. *Cell.* 167: 203–218.e17.
47. O'Brien, R. L., and W. K. Born. 2015. Dermal γδ T cells—what have we learned? *Cell. Immunol.* 296: 62–69.
48. Bordessoule, D., P. Gaulard, and D. Y. Mason. 1990. Preferential localisation of human lymphocytes bearing gamma delta T cell receptors to the red pulp of the spleen. *J. Clin. Pathol.* 43: 461–464.
49. Nolte, M. A., E. N. Hoen, A. van Stijn, G. Kraal, and R. E. Mebius. 2000. Isolation of the intact white pulp. Quantitative and qualitative analysis of the cellular composition of the splenic compartments. *Eur. J. Immunol.* 30: 626–634.
50. Nanno, M., T. Shiohara, H. Yamamoto, K. Kawakami, and H. Ishikawa. 2007. γδ T cells: firefighters or fire boosters in the front lines of inflammatory responses. *Immunol. Rev.* 215: 103–113.
51. Wands, J. M., C. L. Roark, M. K. Aydintug, N. Jin, Y. S. Hahn, L. Cook, X. Yin, J. Dal Porto, M. Lahn, D. M. Hyde, et al. 2005. Distribution and leukocyte contacts of gammadelta T cells in the lung. *J. Leukoc. Biol.* 78: 1086–1096.
52. Carrasco, Y. R., and F. D. Batista. 2007. B cells acquire particulate antigen in a macrophage-rich area at the boundary between the follicle and the subcapsular sinus of the lymph node. *Immunity* 27: 160–171.
53. Cinamon, G., M. A. Zachariah, O. M. Lam, F. W. Foss, Jr., and J. G. Cyster. 2008. Follicular shuttling of marginal zone B cells facilitates antigen transport. *Nat. Immunol.* 9: 54–62.
54. Junt, T., E. A. Moseman, M. Iannacone, S. Massberg, P. A. Lang, M. Boes, K. Fink, S. E. Henrickson, D. M. Shayakhmetov, N. C. Di Paolo, et al. 2007. Subcapsular sinus macrophages in lymph nodes clear lymph-borne viruses and present them to antiviral B cells. *Nature* 450: 110–114.